buildings

MDPI

Article

Impact of Green Roofs and Walls on the Thermal Environment of Pedestrian Heights in Urban Villages

Chang Lin [1] and Shawei Zhang [2,*]

[1] Innovation School of Greater Bay Area, Guangzhou Academy of Fine Arts, Guangzhou 510261, China; linchang@gzarts.edu.cn
[2] School of Architecture & Applied Arts, Guangzhou Academy of Fine Arts, Guangzhou 510261, China
* Correspondence: zhang_shawei@gzarts.edu.cn

Abstract: (1) Background: Urban villages in Guangzhou are high-density communities with challenging outdoor thermal environments, which significantly impact residents' thermal comfort. Addressing these issues is crucial for improving the quality of life and mitigating heat stress in such environments. (2) Methods: This study utilized a validated ENVI-met microclimate model to explore the synergistic cooling effects of roof greening and facade greening. Three greening types—total greening, facade greening, and roof greening—were analyzed for their impacts on air temperature, mean radiant temperature, and physiologically equivalent temperature (PET) at a pedestrian height of 1.5 m under varying green coverage scenarios. (3) Results: The findings showed that total greening exhibited the greatest cooling potential, especially under high coverage (≥50%), reducing PET by approximately 2.5 °C, from 53.5 °C to 51.0 °C, during midday, and shifting the heat stress level from "extreme heat stress" to "strong heat stress". Facade greening reduced PET by about 1.5 °C, while roof greening had a limited effect, reducing PET by 1.0 °C. Furthermore, under coverage exceeding 75%, total greening achieved maximum reductions of 3.0 °C in mean radiant temperature and 1.2 °C in air temperature. (4) Conclusions: This study provides scientific evidence supporting total greening as the most effective strategy for mitigating heat stress and improving thermal comfort in high-density urban villages, offering practical insights for optimizing green infrastructure.

Keywords: roof greening; facade greening; urban villages; outdoor thermal environment; thermal comfort; ENVI-met

Citation: Lin, C.; Zhang, S. Impact of Green Roofs and Walls on the Thermal Environment of Pedestrian Heights in Urban Villages. *Buildings* **2024**, *14*, 4063. https://doi.org/10.3390/buildings14124063

Academic Editor: Apple L.S. Chan

Received: 2 December 2024
Revised: 12 December 2024
Accepted: 18 December 2024
Published: 21 December 2024

1. Introduction

Urban villages are a special product of China's urbanization process, characterized by high building density, high population density, weak infrastructure, and intensive land use [1]. Originally rural, these areas were gradually surrounded by urban centers as cities expanded, but due to the special nature of the land, they were not fully integrated into urban planning, resulting in a situation where residents' self-built houses and temporary rental housing are densely packed, and the population of urban villages is dominated by migrant workers [2]. The reasons for its formation mainly include factors such as the impetus of the urbanization process, differences in the land system, the influx of foreigners, and the driving force of the economic interests of the aborigines [3]. Despite the government's recent renovation policies, high land prices and conflicts of interest with indigenous residents have led to slower progress in the renovation of urban villages, which still maintain their unique built environments.

In recent years, the urban heat island effect has been increasing. Hot and humid areas have high temperatures and high humidity in summer, and the heat island effect superimposed on the hot summer climate poses a serious threat to people's lives and health, a phenomenon that is even more pronounced in urban villages [4]. The most direct and environmentally friendly way to reduce this thermal discomfort is to introduce urban

greening, which consists of greenery planted on the ground [5] and attached to building surfaces [6]. Previous studies have shown that building-attached greening can provide significant thermal effects, such as reducing the amount of solar heat radiation gained by foliage and the ability to convert absorbed solar heat into latent heat through transpiration, which ultimately leads to lower building surface temperatures [7–9].

Previous research on green infrastructure has focused on the impacts of trees in cities; however, the impacts of trees occur primarily below the canopy [10]. The high-density building layout of urban villages results in very limited areas where large trees can be planted, so large trees are not the best choice in urban villages. Building-attached greenery is more suitable for placement in urban villages than trees. Building-attached greenery mainly consists of green roofs and green walls, and their cooling effects on the outdoor environment and surface temperature have been extensively studied by simulation and measurement methods. Table 1 lists articles and results on the cooling effects of green roofs and green walls.

Table 1. Review related to the cooling effect of green roofs and walls.

Author	Location	Climate	Type	Scale	Findings
Alexandri and Jones et al. [11]	Mumbai, India	Hot and humid	Green roofs and green walls	Air temperature reduction	Average cooling effect of 9.1 °C in hot and dry environments, 6.9 °C in hot and humid environments
Hien et al. [12]	Singapore	Hot and humid	100% green wall coverage	Air temperature reduction	0.3 °C reduction with 100% green wall coverage
Marina et al. [13]	Spain	Mediterranean	Green walls	Air temperature reduction	Maximum cooling effect of 2.9 °C
Morakinyo et al. [14]	Hong Kong	Hot and humid	Green walls	Air temperature reduction	50% green wall coverage required to reduce air temperature by 1 °C
Tan et al. [15]	Nagoya, Japan	Hot and humid	Green walls	Localized cooling at 1.0 m	Maximum cooling effect at 1.0 m from the wall
Onishi et al. [16]	Nagoya, Japan	Hot and humid	Rooftop lawn	Surface temperature reduction	Cooling effect ranges from 2 °C to 4 °C
Taiwan experiment [17]	Taiwan	Hot and humid	Rooftop lawn	Outdoor cooling and internal energy demand	Rooftop lawn contributes to outdoor cooling and reduces internal energy demand
Scherba et al. [18]	Portland, Oregon	Mediterranean	Green roof vs. black roof	Sensitive heat flow reduction	50% reduction in sensitive heat flow compared to black roof

Alexandri and Jones et al. [11] modeled the cooling effects of green walls and roofs in urban canyons across various climates, finding reductions of 9.1 °C in hot-dry and 6.9 °C in hot-humid environments. Hien et al. [12] reported a 0.3 °C temperature drop with 100% green wall coverage in Singapore, while in Spain's Mediterranean climate, green walls reduced temperatures by up to 2.9 °C [13]. Morakinyo et al. [14] found that 50% green wall coverage in Hong Kong lowered temperatures by 1 °C, and Tan et al. [15] observed the greatest cooling effect at 1.0 m from the wall in Japan. Other studies highlighted benefits of rooftop greenery, including a 2–4 °C cooling effect in parking lots [16], reduced energy demand in Taiwan [17], and a 50% reduction in heat flow in Portland's Mediterranean climate [18]. These studies surface that building-attached greening can effectively improve the thermal environment of the building's outdoor environment.

However, although a large number of studies have examined the cooling effect of building-attached greenery, most of these studies have focused on low-density, mono-functional urban environments or specific climatic zones, and there is a lack of systematic research on high-density urban villages, which are a complex urban form [19–21]. Urban villages differ significantly from traditional urban environments due to their unique building densities, land uses, and social structures, and the findings of existing studies may not be directly applicable to such high-density areas [22,23]. Therefore, in this study, the effect of building-attached greening in the high-density environment of urban villages in Guangzhou City is explored in depth, and the ENVI-met microclimate prediction model is utilized to accurately study the effects of green roofs and green walls on the

outdoor thermal environment of urban villages, and the cooling effects of different types of building-attached greening coverage are systematically analyzed.

In addition to the above parts, this study makes some new contributions. Theoretically, it reveals the variation and synergistic cooling effects of rooftop greening and green walls over time under different cover conditions, especially in high-density environments. In terms of application, this study extends the scope of the cooling effect of building-attached greenery to the community scale, providing practical insights for urban planners to optimize greening strategies targeting dense urban forms such as urban villages. These contributions set this study apart from previous work and emphasize the relevance of this study in addressing urban thermal challenges in unique and under-explored settings.

2. Materials and Methods

This study consists of two main phases designed to comprehensively analyze the impact of building-attached greenery on the outdoor thermal environment in high-density urban villages.

Phase 1: This phase involved detailed field measurements and data collection to establish the baseline environmental conditions of the study site. Specific activities included measuring key thermal parameters such as air temperature, mean radiant temperature, and humidity at various points across the site. The measurement locations were then accurately recreated using 3D modeling tools to reflect the real-world conditions in the simulation environment. The data collected from these field measurements were subsequently used to validate the ENVI-met model.

Phase 2: Building upon the validated model, a comprehensive parametric study was conducted to investigate the effects of varying coverage and forms of building-attached greenery on the outdoor thermal environment. A total of 60 scenarios were designed, combining different levels of green coverage (ranging from 5% to 100% at 5% intervals) and three greening forms: total greening, facade greening, and roof greening. These scenarios enabled a systematic exploration of the cooling potential of different greening strategies under various coverage conditions. The detailed methodological framework, including the configuration of scenarios and modeling approach, is illustrated in Figure 1.

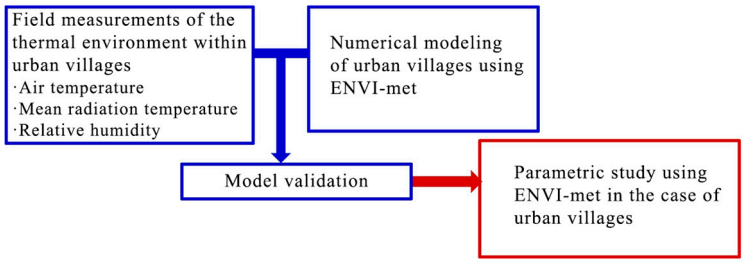

Figure 1. Methodological framework for the study.

2.1. Field Measurement Campaign

This study was conducted on 30 July 2024 from 8:00 to 18:00 h in an urban village in Panyu District, Guangzhou City, whose location map and on-site measurement scene are shown in Figure 2. The community is densely arranged with buildings occupying more than 90% or more of the space, with sparse open space and green areas, and less than 5% of the community is green. The spacing between buildings is usually less than 3 m, and some buildings are seamlessly connected, resulting in poor air circulation and lighting conditions within their communities. Road widths are generally narrow, with main lanes ranging from approximately 3–5 m wide and secondary lanes less than 3 m for pedestrian traffic only. The thermal environment in the community is further exacerbated by the fact that the community's underlayment materials are mainly building structures made of cement and bricks, and the roofs are mostly waterproof-treated cement boards and iron sheets, with

some buildings using simple colored steel sheet roofs. Thus, making it an ideal site for this study.

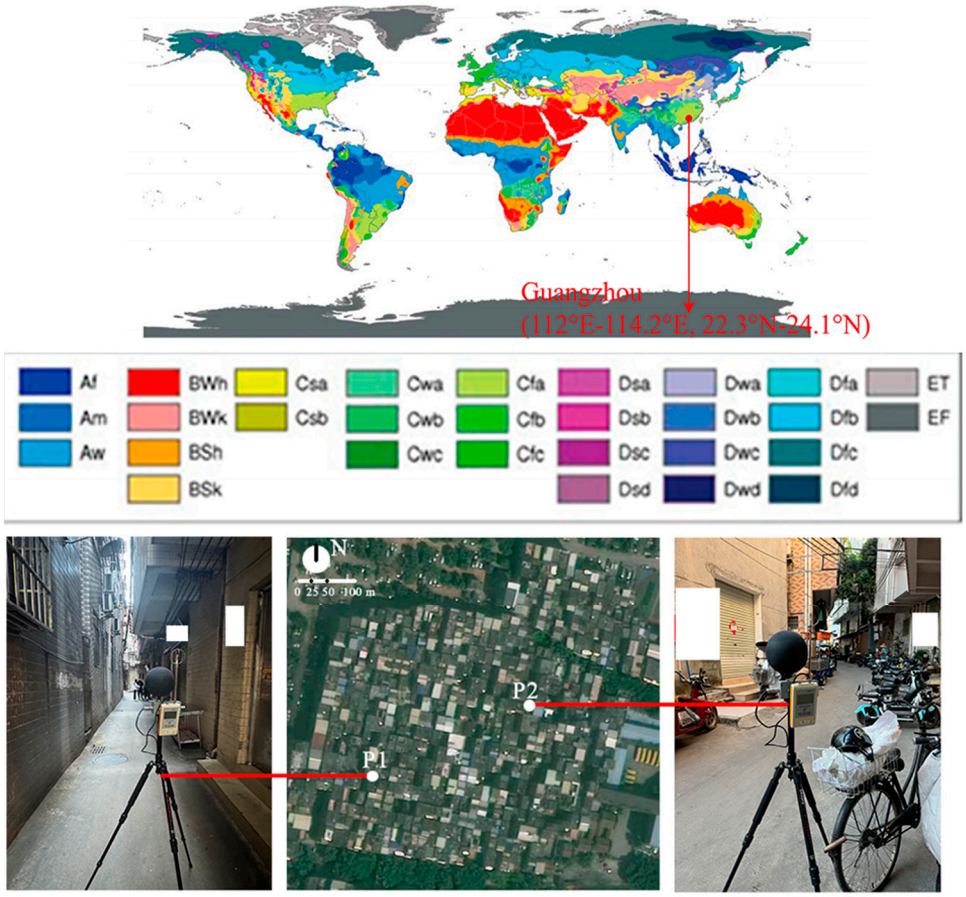

Figure 2. Research area.

In this study, a TJHY-SSDZY-1 Thermal Comfort Instrument (Beijing, China, Tianjian Huayi Technology Development Co., Ltd.) was used to measure the thermal environment (air temperature, relative humidity, wind speed, and black sphere temperature) at four points in this community, and all the instruments were arranged at a distance of 1.5 m from the ground, and the environmental parameters were recorded once every 30 s [24], and the specific parameters of the experimental equipment are shown in Table 2.

Table 2. Instruments and technical parameters.

Instrument	Parameter	Range	Accuracy	Sampling Rate
SSDZY-1	Air temperature	−20–80 °C	±0.3 °C	30 s
	Relative humidity	−99.9%	±2% (10–90%)	
	Globe temperature	−20–80 °C	±0.3 °C	
	Wind speed	0.05–5 m/s	5% ± 0.05 m/s	

In order to objectively evaluate the comfort level of a space, the thermal index usually includes four basic physical parameters: air temperature, relative humidity, wind speed, and average radiant temperature, which is calculated as shown in Equation (1) [25]. Of these, the mean radiant temperature is the most important for the widely used thermal index (Physiologically Equivalent Temperature, PET) [26]. PET is an indicator of thermal comfort derived from human heat balance models and is widely used to assess the outdoor thermal comfort of urban residents [27,28]. In this study, PET values were calculated using

the BIO-met module of the ENVI-met model to assess outdoor human thermal comfort. The PET derived from the BIO-met module is the same as the PET calculated using Höppe's PET Fortran program. The thermal resistance of clothing is defined as 0.25 clo, and the calculation body is an adult of 35 years old, 170 cm in height and 60 kg in weight. In this study, the evaluation range of PET in Guangzhou was selected, and the specific thermal stress level is shown in Table 3 [29].

$$Tmrt = \left[\left(T_g + 273 \right)^4 + \frac{\left(1.1 \times 10^8 \times V_a^{0.6} \right)}{\left(\varepsilon_g \times D^{0.4} \right)} \times \left(T_g - T_a \right) \right]^{\frac{1}{4}} - 273, \quad (1)$$

where D represents a black sphere thermometer with a diameter of 0.15 m and εg represents a radiant emissivity of 0.95. Tg is the black sphere temperature, Ta is the air temperature, and Va is the wind speed.

Table 3. Thermal sensation of different thermal stress categories and PET.

Different Profit Categories and PET Thermal Sensation in Guangzhou Area		
-	very cold	extreme cold stress
-	cold	strong cold stress
≤11.3 °C	cool	moderate cold stress
11.3–19.2 °C	slightly cool	mild cold stress
19.2–24.6 °C	comforts	neutral
24.6–29.1 °C	slightly warm	mild hot stress
29.1–36.3 °C	warm	moderate hot stress
36.3–53.6 °C	hot	strong hot stress
≥53.6 °C	very hot	extreme hot stress

2.2. Numerical Modeling of Measurement Locations

Before proceeding to the second phase of the study, the performance of the ENVI-met model needs to be evaluated [30,31]. Therefore, this study constructed an ENVI-met current state model that includes the study area and its surroundings. That is, the modeled buildings, the greenery in and around the site, and the subsurface materials were included. The simulated and measured values of the model were compared and evaluated. This section focuses on the ENVI-met simulation model.

Description of the ENVI-Met Model

ENVI-met is a three-dimensional computational fluid dynamics (CFD) model that uses a standard k-ε turbulence model to solve the Reynolds-averaged Navier–Stokes (RANS) equations [32]. The model is capable of simulating the interactions between surface, vegetation, and the atmosphere in complex urban environments of different shapes, heights, and materials, covering the road and surface characteristics of a wide range of materials and vegetation configurations [33]. ENVI-met uses high-resolution spatial (0.5–10 m) and temporal (up to 10 s) grids for simulation, thus enabling in-depth analysis of small-scale interactions between individual buildings, surfaces, and plants [34]. In this model, plants (e.g., trees and grasses) are viewed not only as permeable media for wind flow and sunlight exposure, but also as actively interacting with their surroundings through energy absorption and evaporation [35]. Furthermore, with the additional software ALBERO, trees can be modeled as three-dimensional complex elements. In order to realize this, the vertical and horizontal profiles of the leaf area density (LAD) as well as the structure of the horizontal canopy must be known in advance [36].

ENVI-met version 5.6.1 features significant enhancements in vertical greening simulation, allowing more accurate simulation of urban greening systems such as green facades and green walls [37]. This version enables vertical greening plants to exhibit actual growth patterns in space by means of an improved 3D plant model that takes into account the leaf area density distribution, vertical growth characteristics, and canopy structure of the plant. At the same time, this version further enhances the interaction between plants and walls and is able to simulate the shading effect of plants, evapotranspiration, and their thermal and humidity regulation impacts on the wall and the surrounding environment. In addition, the model optimizes the water and energy exchange process to accurately simulate plants regulating wall heat and humidity through transpiration and evaporation and interacting with ambient temperature, humidity, and light conditions. The new version also supports more complex vertical greening configurations, such as different plant layers and species combinations, enabling more flexible simulation of the effects of different materials and vegetation combinations on thermal effects and air flow.

2.3. Model Validation: Simulation Setup at the Measurement Site

The community model for this study was developed based on the Geographic Information System and the dimensions of the building and street layouts obtained from the field survey. The simulation area is 246 m × 231 m with a grid of 3 m both horizontally and vertically. In this study, the heights of the buildings range from 6–21 m, and their surface materials are dominated by brick walls and concrete, while the streets in the community are mainly covered by concrete and asphalt. In terms of plants, the large trees in the community were modeled using the characteristic parameters of typical trees in Guangzhou City, with the following physical parameters: tree height of 10 m, crown spread of 8 m, height under branches of 2 m, and foliage short-wave reflectance of 18% [38]. For initialization of the simulation, meteorological records (air temperature, relative humidity, wind speed, and wind direction) on the measurement date (30 July 2024) were obtained from the meteorological station in Panyu District, Guangzhou City, as the climatic boundary conditions for the simulation of the corresponding date, and the summary information of the ENVI-met inputs is shown in Table 4.

Table 4. Summary of input, test parameters, and corresponding values for validation simulation.

Parameter	Definition	Input Value
Meteorological	Initial air temperature (°C)	Hourly profile
	Relative humidity (%)	Hourly profile
	Inflow direction	135°
	Wind speed at 10 m (m/s)	2.2 m/s
	Soil temperature (°C)	25
Building information	Building and wall height (m)	6–21
	Bare wall, road and roof albedo	0.3
Plant information	Plant type	Original trees
	Leaf area density (m^2/m^3)	1.92
	Plant albedo	0.18
	Height of plant (m)	10
	Weight of plant (m)	8
Grid settings	Number of grids	82 × 77 × 15
	Grid size	3 m × 3 m × 3 m

Root Mean Square Error (RMSE), Mean Absolute Error (MAE), and Coefficient of Determination (R^2) are widely recognized evaluation metrics, each with distinct advantages and limitations in model evaluation, as extensively discussed in the literature. Given that these metrics differ in their calculation methods and focus, employing a combination of them provides a more comprehensive assessment of the reliability of the simulated data. In studies examining the thermal environment of humid-hot regions, RMSE, MAE, and R^2 are commonly utilized to validate the performance of the ENVI-met 5.6.1 software [5,32,33].

Accordingly, this study adopts these metrics to evaluate and validate the simulation results. The formulas are shown in Equations (2) and (3).

$$\mathrm{RMSE} = \sqrt{(\Sigma(\mathrm{O_i} - \mathrm{P_i})^2/\mathrm{n})} \quad (2)$$

$$\mathrm{MAE} = \Sigma\,|\,\mathrm{O_i} - \mathrm{P_i}\,|\,/\mathrm{n} \quad (3)$$

where O_i is the observed value, P_i is the simulated value, and n is the number of samples. The smaller the value, the more accurate the simulation result.

2.4. Parametric Studies: Model Setup and Scenario Development

In the second phase of this study, a total of 60 parametric scenarios were developed to understand the effect of greening attached to buildings of different types of densities on community air cooling and thermal comfort, and in this section, the model setup, configuration, and initialization of input values for the study are fully described.

2.4.1. Setting of the Parametric Study

The parametric study is based on typical community patterns in Guangzhou City, with Panyu District in particular as a case study. This area is an important part of Guangzhou city, and its resident population is about 2.66 million with a population density of 14,000 people/km^2 [39]. The study did not alter the building materials, underlayment materials, or original vegetation in the community, resulting in a total of 60 simulated scenarios:

In this study, building-attached greening was categorized into two forms: green roofs and green walls, and as a result, three greening arrangement schemes were formed: (1) green roofs only; (2) green facades only; and (3) containing both green roofs and green facades. In addition to this, this study further parameterized the green facade based on its ratio of total green facade area to total building surface area to form a proportion of green coverage starting at 5% and ending at 5% intervals to 100% for a total of 20 scenarios. These case studies were designed to determine the amount of greening (i.e., green coverage) needed to improve the outdoor thermal environment for different combinations of building-attached greening forms, while the uniform coverage assumption provides a standardized research basis for the model. This approach helps to reveal the potential regulatory mechanisms of different coverage and greening forms and thus provides a theoretical reference for complex practical scenarios. The specific scenarios are shown in Figure 3. The red color of the building plan models indicates that they were added with building-attached greenery. At the end of the simulation, the average values for the whole urban village in each scenario were analyzed. During this phase, additional soil-based green facades and green roofs were also introduced with the parameters shown in Table 5. The simulation time was from 8:00 to 18:00 to represent the cloudless summer weather during the day.

Table 5. Plants selected for green roofs and green walls.

Parameter	Definition	Input Value
Greening properties	Leaf area index (m^2/m^2)	1.50
	Leaf angle distribution (0–1)	0.50
Substrate properties	Emissivity of substrate (0–1)	0.95
	Albedo of substrate (0–1)	0.30
	Water coefficient of substrate for plant (0–1)	0.50
	Air gap between substrate and wall (m)	0.10

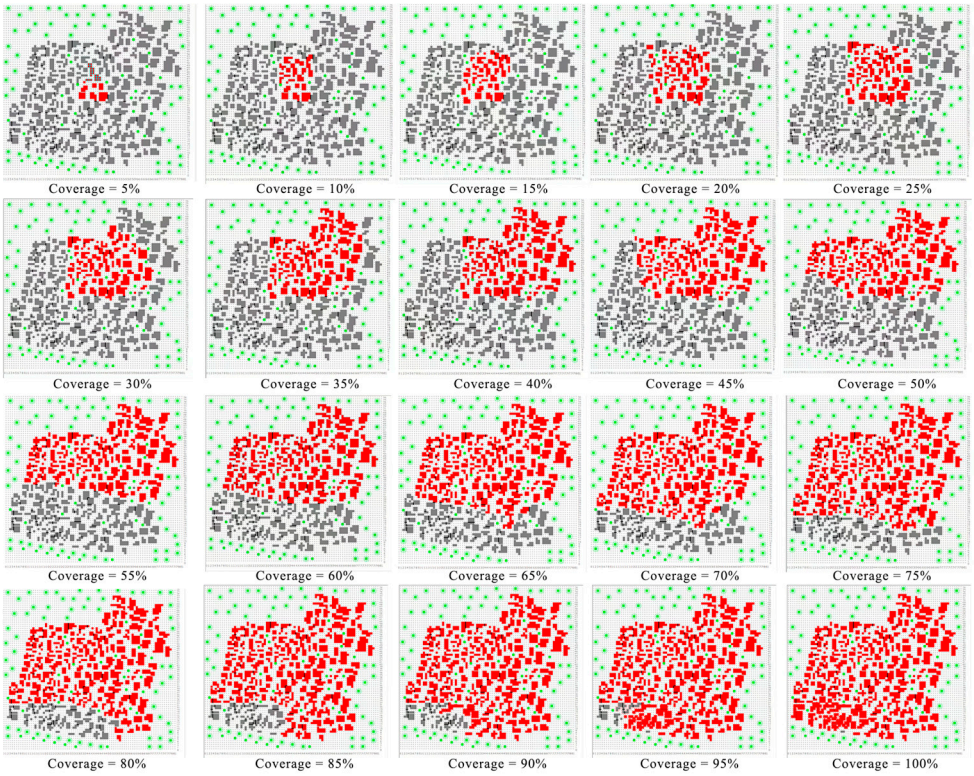

Figure 3. Simulation schemes in parametric studies.

2.4.2. Parametric Model Initialization

To initialize the model for this study, the air temperature and relative humidity for each hour of the measurement day were placed at the model boundary using a simple forcing method. This method is able to reduce the error caused by the boundary conditions and has a faster computation speed. The input minimum and maximum air temperatures were 40.3 and 27.1 °C, respectively, and the relative humidity was 45.3–71.6%. In addition to this, the wind at 10 m above the ground was 2.2 m/s and the direction of the airflow was 135°, which is a direction that can represent the dominant wind direction in the summer in Guangzhou City. The soil temperature was set to 25 °C. The building information and the information of the subsurface in the community are consistent with the parameters in Section 2.3.

3. Results and Discussion

3.1. Comparison Between Simulated and Measured Data

A comparison of measured and simulated results for air temperature, relative humidity, and mean radiation temperature at Monitoring Point 1 and Monitoring Point 2 in the community is shown in Figure 4. In terms of air temperature, the R^2 of Point 1 and Point 2 are 0.9837 and 0.9821, the MAE is 0.9597 °C and 0.9578 °C, and the RMSE is 1.0176 °C and 1.0762 °C, which indicate that the simulation model captures the trend of air temperature more accurately. For relative humidity, the R^2 of Point 1 and Point 2 are 0.9801 and 0.9821, the MAE is 0.7681% and 0.8086%, and the RMSE is 0.9598% and 1.1704%, which indicates that the model also has a high simulation accuracy in relative humidity. For the mean radiation temperature, the R^2 of Point 1 and Point 2 are 0.9710 and 0.9777, the MAE is 1.9434 °C and 1.3794 °C, and the RMSE is 2.3485 °C and 4.0203 °C, respectively. Although there are some deviations in the complex radiation environment simulated by the model, in general these results show that the simulation model used is a good reflection of the real situation in the study area [40–42].

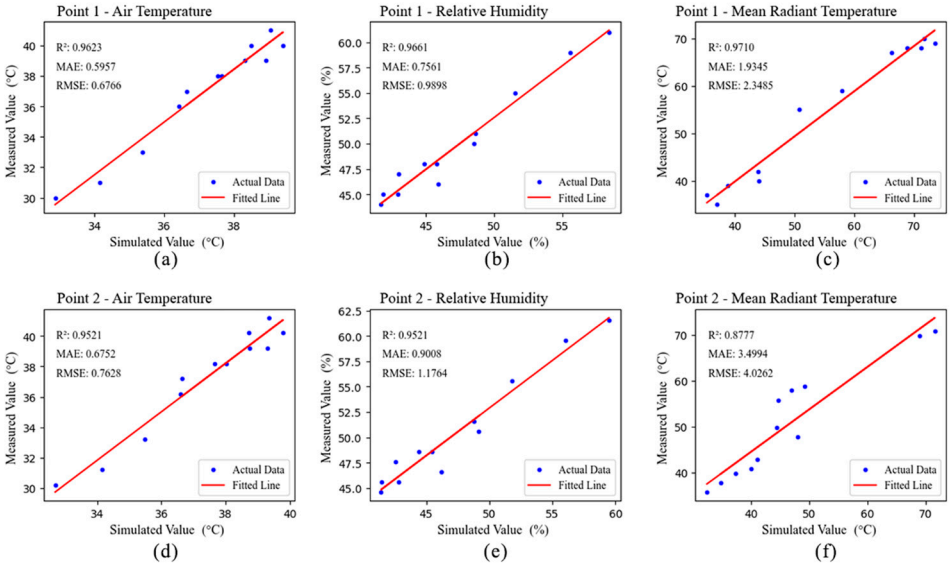

Figure 4. Comparison of analog and measurement: (**a**) air temperature at point 1; (**b**) relative humidity at point 1; (**c**) mean radiation temperature at point 1; (**d**) air temperature at point 2; (**e**) relative humidity at point 2; (**f**) mean radiation temperature at point 2.

3.2. Results of the Parametric Study

Due to the large number of working conditions in this study, and to enhance the readability of the article, the results in this section are intercepted with the average value of each parameter within the whole community and expressed in the form of a line graph.

3.2.1. Air Temperature

The effect of different green coverage and green types on air temperature in the community is shown in Figure 5. During the simulation period, the variation of air temperature showed a clear regularity, and its daily trend showed a trend of highest temperatures at noon and lower temperatures in the morning and evening for all coverage conditions. However, the moderating effects of cover and greening type on temperature varied across time periods and cover levels. At low cover (5–30%), the difference in cooling among the three greening types was small, with the ALL type only about 0.2 °C cooler than the FACADE and ROOF types at midday, suggesting that the influence of greening type is more limited under lower cover conditions, with the cooling effect being more dominated by the natural environment [43]. Under medium coverage (35–70%), the differences between the greening types began to appear, especially the cooling effect of the ALL type gradually increased, and its midday temperature was about 0.5 °C lower than that of the ROOF. When the coverage reached more than 50%, the cooling effect of the ALL type showed more stable performance, especially at the peak time of midday temperature; its cooling ability was significantly better than the other two greening types. The advantage of the ALL type is even more pronounced under high coverage (75–100%) conditions, with peak midday temperatures of about 37.0 °C at 100% coverage, which is 0.8 and 0.5 °C lower than ROOF and FACADE, respectively. The cooling effect of total greening is significantly enhanced at high cover. This result is consistent with the findings of previous researchers, but the cooling effect of 100% green coverage of individual buildings in this study was 0.6 °C higher than in Singapore [12]. The cooling effect of comprehensive greening is significantly enhanced at high coverage. In addition, it can be observed from the time-by-time change graph that the cooling effect is not only reflected in the high temperature at midday, but also the temperature difference between morning and evening gradually widens with the increase of the coverage. At low coverage (5–30%), the temperature change profiles of ALL, FACADE, and ROOF types nearly overlap, but as coverage increases (75–100%), the ALL type begins to show a cooling effect in the morning and evening hours, with a gap of 0.3 °C

between it and the other types. This suggests that full-scale greening with high cover can provide more significant temperature regulation across the all-weather range, whereas the cooling effect of facade and roof cover only is more confined to the midday hours, with a more limited ability to regulate in the morning and evening.

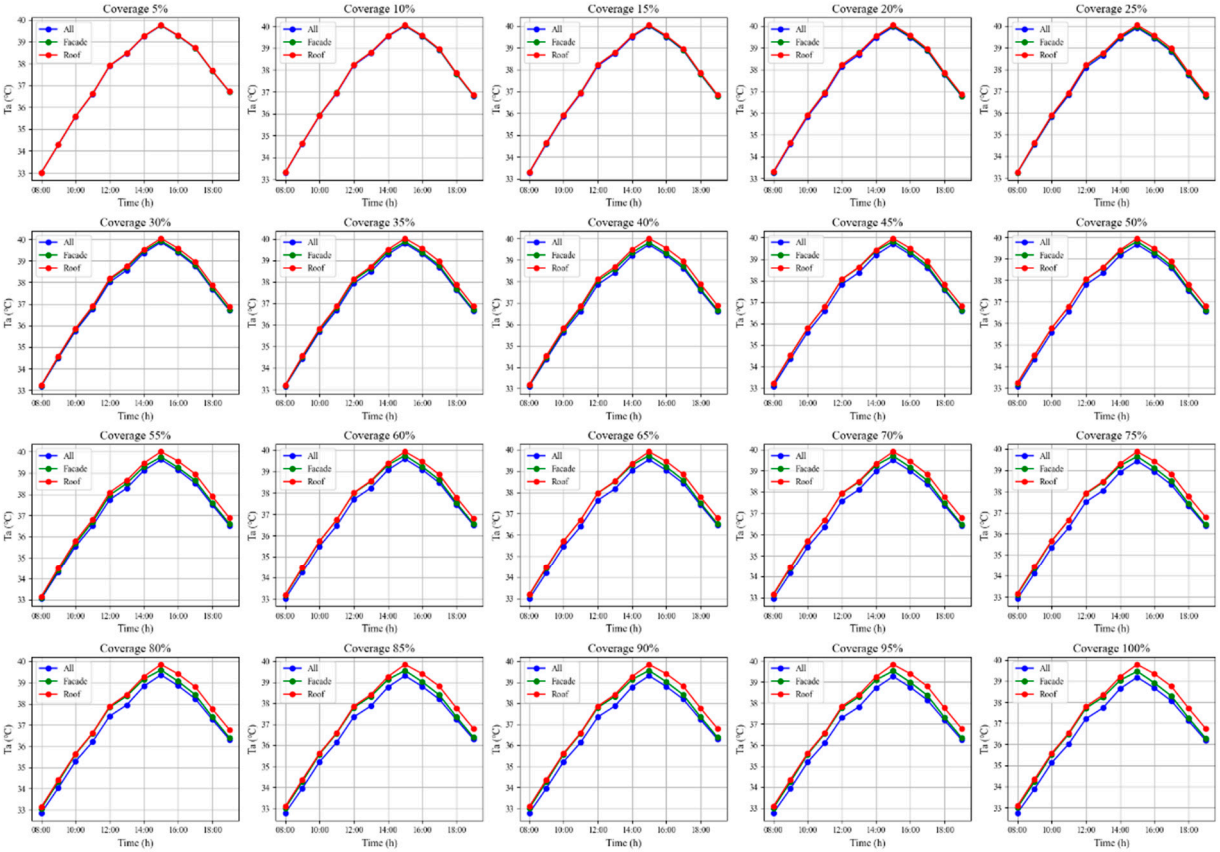

Figure 5. Effects of greening forms on the air temperature of communities with different percentages of coverage.

The results of the time-by-time variability analysis of air temperature are shown in Figure 6, which shows that there are significant differences between the different greening forms, especially between all-greening and roof greening and all-greening and facade greening, with *p*-values lower than 0.05 at all-time points. This suggests that the all-greening form is more effective in cooling the air temperature than the other two greening forms. The cooling effect of all-greening was particularly significant during the morning and midday hours (8:00–12:00), with *p*-values ranging from 0.001 to 0.016. In contrast, the differences between facades and roofs were not statistically significant at most time points (e.g., $p > 0.05$ at 8:00 and 9:00), suggesting comparable performance. Overall, all forms of greening significantly reduced temperatures, especially during the morning and midday heat hours.

The overall regression relationship between coverage and air temperature is shown in Figure 7. In terms of the overall relationship between cover and temperature, this graph clearly shows the significant moderating effect of the three greening types on the temperature at 1.5 m of pedestrian height as cover increases, as well as the significant differences between the types. The regression curves and shaded areas in the figure indicate the trend and margin of error of the average temperature for the three types, respectively. The ALL type shows the most significant downward trend in temperature as coverage increases, with an average of about 0.4 °C corresponding to each 20% increase in coverage. At 100% cover, ALL types reduced temperatures from 37.9 °C at low cover to 36.7 °C, demonstrating the significant cooling potential of total greening under high

cover conditions. The source of this effect is mainly the combined coverage of horizontal and vertical surfaces by comprehensive greening, which reduces the absorption of thermal radiation from roofs and walls, while significantly improving the local thermal environment through evapotranspiration [44,45]. Compared to the ALL type, the FACADE type had the next best cooling effect. As the percentage of coverage increased from 5% to 100%, the temperature dropped by about 0.8 °C on average (from 38.0 °C to 37.2 °C). This effect was mainly due to the effective suppression of heat radiation from the building facade, as well as the increased evapotranspiration effect of the green wall, which had a more direct effect on the air temperature near the surface [46,47]. It is worth noting that the cooling capacity of FACADE is relatively limited under low to medium coverage conditions, but its cooling trend begins to accelerate at coverage levels above 50%. This suggests that vertical greening can only fully demonstrate its ability to improve air temperatures at pedestrian heights at higher coverages. In contrast, the ROOF type had the most limited cooling effect, with a relatively flat temperature profile, with each 20% increase in coverage resulting in a temperature drop of only about 0.2 °C. At 5% coverage, ROOF had a temperature of 38.1 °C, only 0.1 °C higher than the FACADE type and 0.2 °C higher than the ALL type, and at 100% coverage, the ROOF type dropped to a temperature of 37.5 °C that was still higher than the FACADE and ALL types. This phenomenon can be explained by the fact that green roofs affect the indoor environment mainly by reducing the heat load of the roof, and they have a more indirect effect on the improvement of air temperature at a height of 1.5 m [48]. Meanwhile, although the evapotranspiration effect of the green roof has some impact on the environment, the evapotranspiration effect has a weaker effect on the air temperature regulation at the pedestrian height due to its higher location [49].

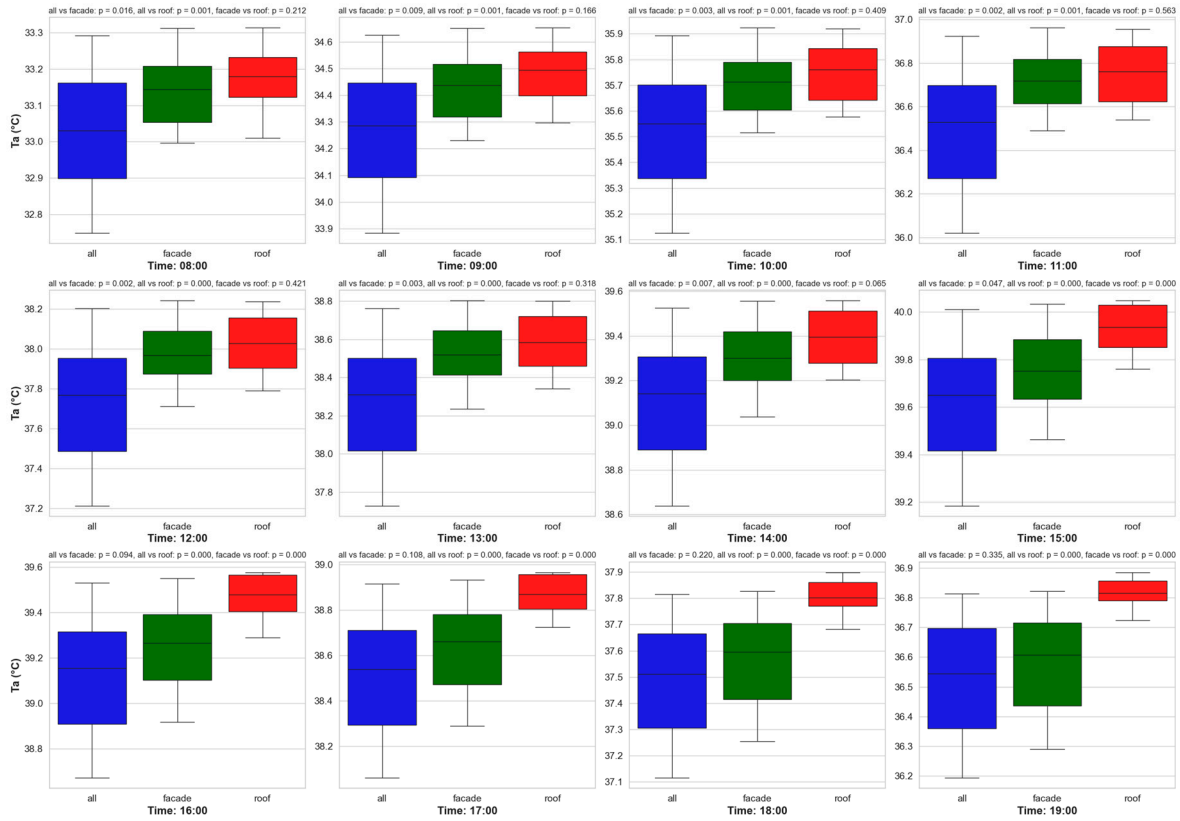

Figure 6. Variability analysis of air temperature in different greening types.

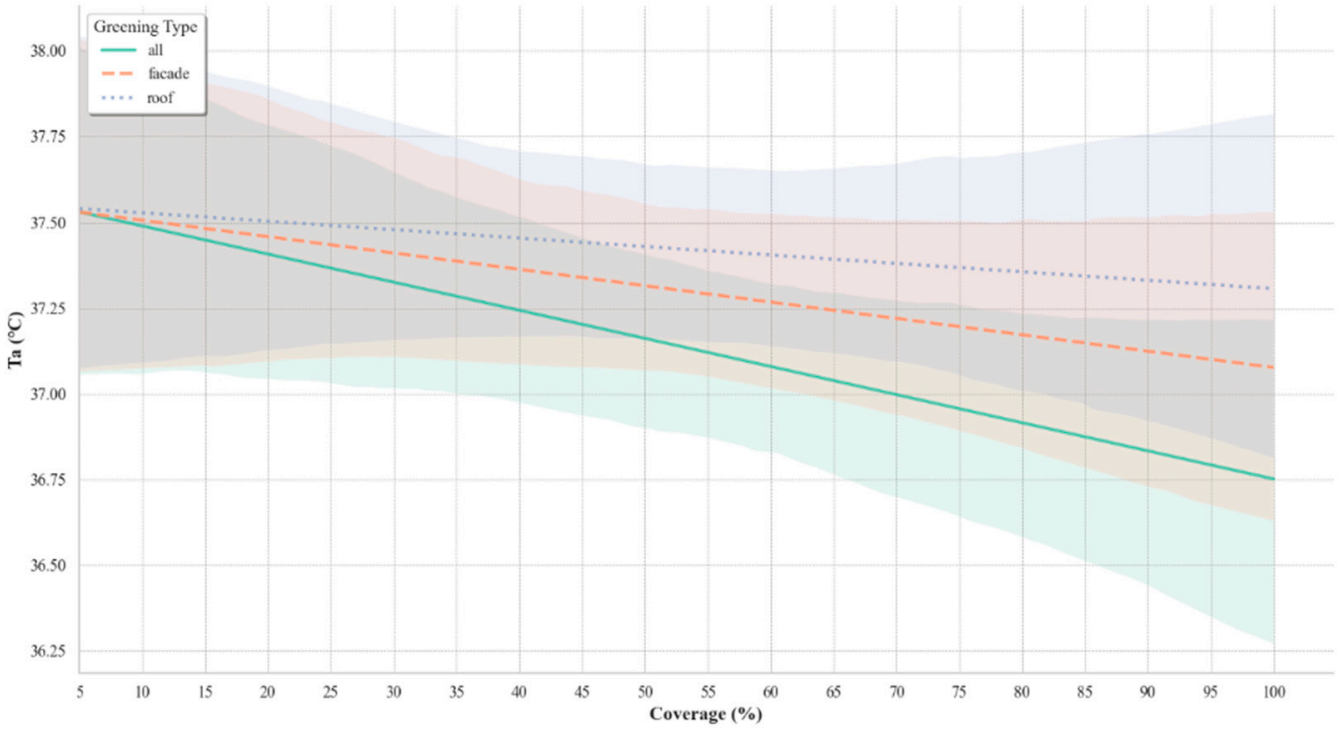

Figure 7. Air temperature levels with regression.

3.2.2. Mean Radiation Temperature

The effect of different green coverage and green types on the mean radiant temperature in the community is shown in Figure 8. Overall, mean radiation temperatures were lower in the morning and evening (08:00 and 18:00) and peaked at midday (12:00–14:00), a pattern that was consistent across all coverage conditions. However, differences in cover and type of greening made the differences in regulatory capacity particularly significant during the midday heat. Under low-coverage (5–30%) conditions, the three greening types regulate mean radiant temperature more closely, with largely overlapping curves. Taking 5% coverage as an example, the mean radiant temperature during the midday hours was about 75.2 °C, and the cooling effect of the ALL type was only about 0.3 °C lower than that of FACADE and ROOF, suggesting that greening under low-coverage conditions is not sufficient to significantly reduce the absorption of radiant heat, and that the evapotranspiration effect is more limited in its scope and intensity. Under moderate cover (35–70%), differences between green types began to emerge. ALL types exhibited more significant cooling effects during the midday hours, with mean radiant temperature of about 1.2 °C lower than roof and 0.6 °C lower than facade. The FACADE type, due to its direct coverage of the wall, has an improved ability to regulate the hot midday hours compared to the roof, but its advantages are still not obvious due to the lack of synergy from green roofs. The advantage of ALL types was further amplified under high cover (75–100%) conditions, with significant regulation throughout the day, especially during the high midday heat, when its mean radiation temperature was reduced to about 65.3 °C, compared to 66.2 °C and 67.4 °C for FACADE and ROOF, respectively. In addition, ALL types also show a more pronounced cooling effect in the morning and evening hours, which is about 0.8 °C and 0.5 °C lower compared to ROOF and FACADE, respectively. The results of mean radiation temperature indicate that full-scale greening not only exerts a strong cooling effect in the midday heat hours, but also improves the radiative environment throughout the day and the overall seeming and air temperature trends.

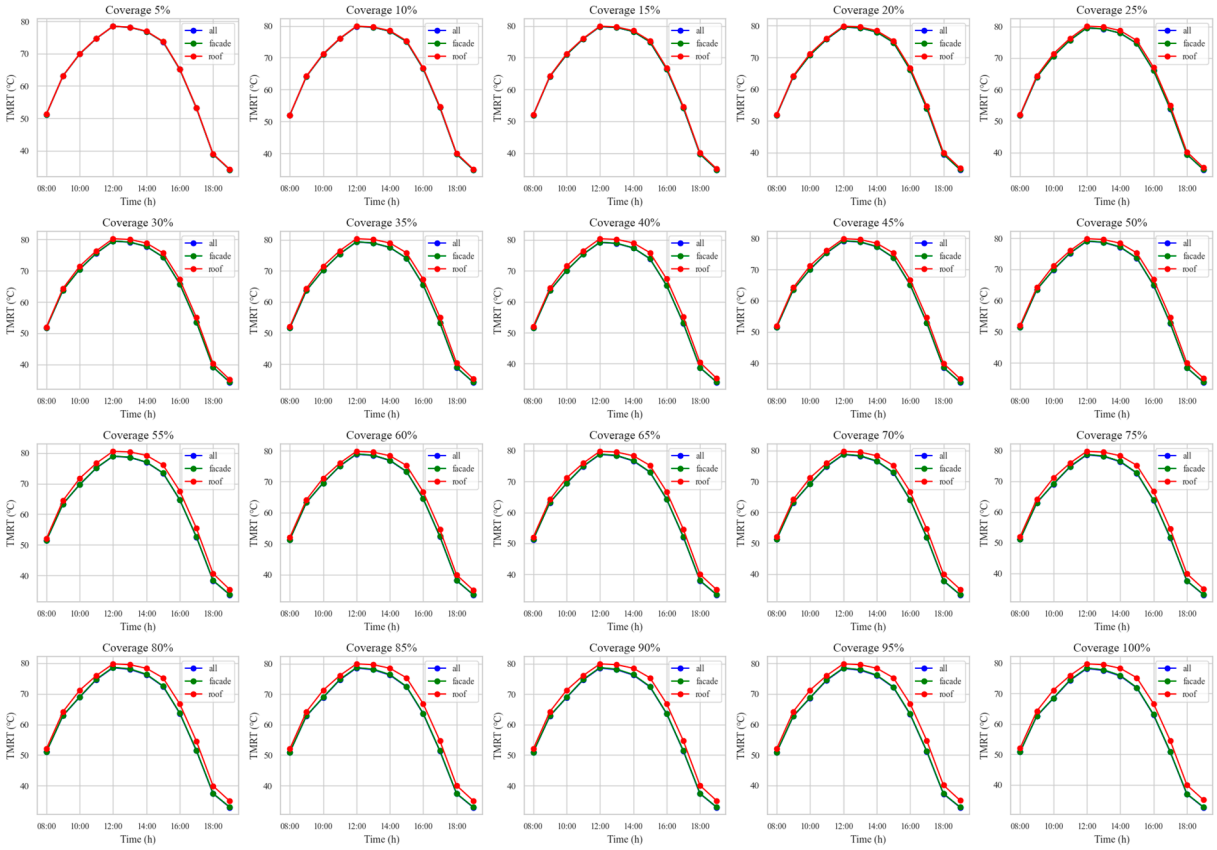

Figure 8. Effects of greening forms on the mean radiation temperature of communities with different percentages of coverage.

The analysis of the variability of the mean radiant temperature on a time-by-time basis is shown in Figure 9. In terms of mean radiant temperature, the comparison of full greenery with green roofs yielded highly significant *p*-values ($p < 0.01$) at all time points, highlighting the effectiveness of the full greenery form of mitigation in terms of radiant heat. The cooling effect was most pronounced during the midday and afternoon hours (12:00–16:00), during which the full-coverage greening was effective in reducing heat radiation from the roof and exterior walls. Comparisons between full coverage and facades showed moderate significance at certain times of day (e.g., *p*-values close to 0.05 at 10:00 and 14:00), suggesting some overlap in performance between the two forms. However, the difference between the facade and roof were limited, with *p*-values not significant ($p > 0.05$) at most time points. This suggests that while facades provide better heat mitigation than roofs, neither can match the combined benefits of all greening.

The overall regression relationship between coverage and mean radiant temperature is shown in Figure 10. The general trend shows a decreasing trend in average radiant temperatures for both ALL and FACADE types as coverage increases from 5% to 100%, with a less pronounced decreasing trend for ROOF. The ALL type demonstrated the best cooling effect, with an average decrease in mean radiant temperature of about 3 °C on average with increasing coverage from 5% to 100%, especially after the coverage exceeded 50%. In contrast, the FACADE type showed a slightly weaker cooling effect than the ALL type, with an average decrease in mean radiant temperature of 2.2 °C (from 67.5 °C to 65.5 °C) with increasing coverage. This effect stems primarily from the fact that vertical greening reduces wall heat radiation, but it does not perform as well as ALL types overall due to the inability to regulate the heat load on the roof. The cooling trend of the FACADE type starts to accelerate after more than 50% coverage, suggesting a gradual release of its potential under high coverage conditions. The ROOF type has the weakest cooling effect, with the average radiant temperature decreasing by only about 1 °C (from 68 °C to 67 °C)

when coverage is increased from 5% to 100%. This suggests that green roofs have limited modulation of thermal radiation at pedestrian heights. Since the evapotranspiration effect of green roofs is mainly concentrated in higher spaces, this also leads to a significantly lower cooling effect than the other two greening types [50].

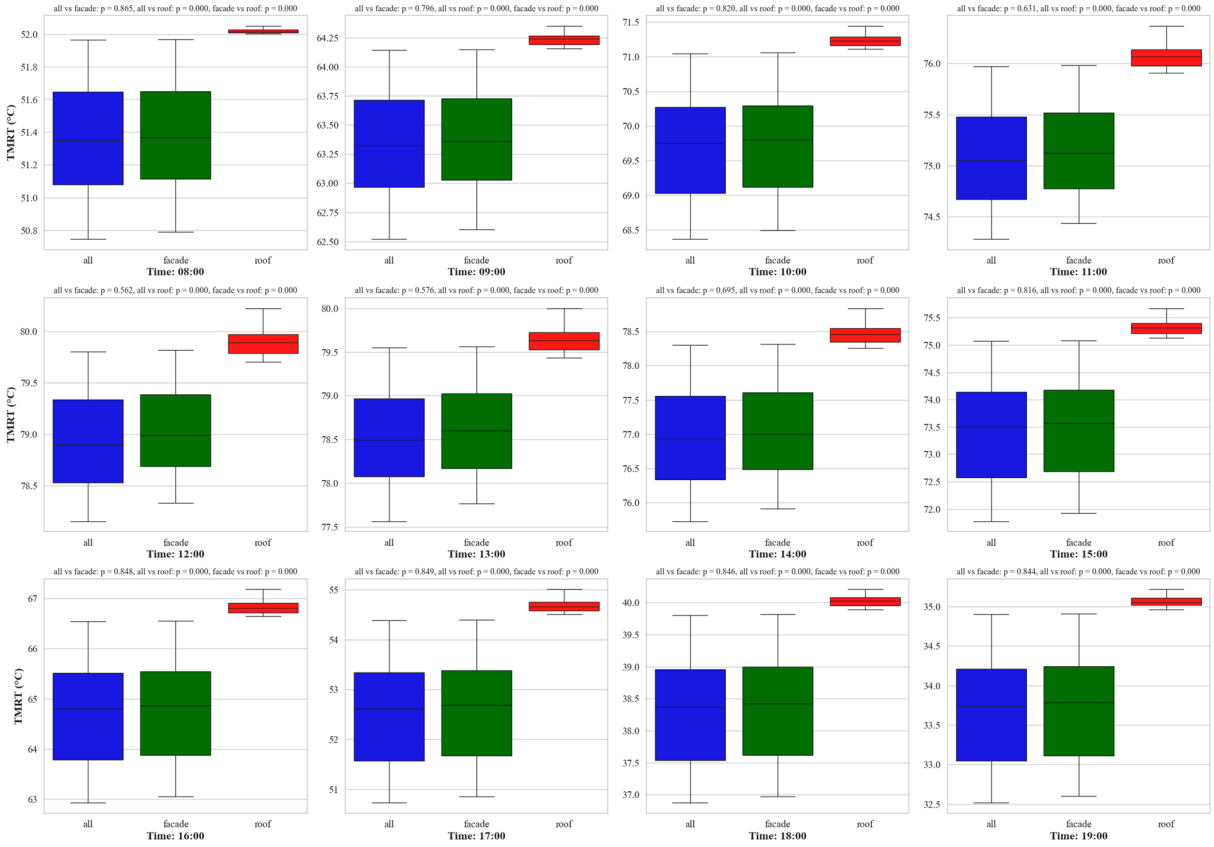

Figure 9. Variability analysis of mean radaition temperature in different greening types.

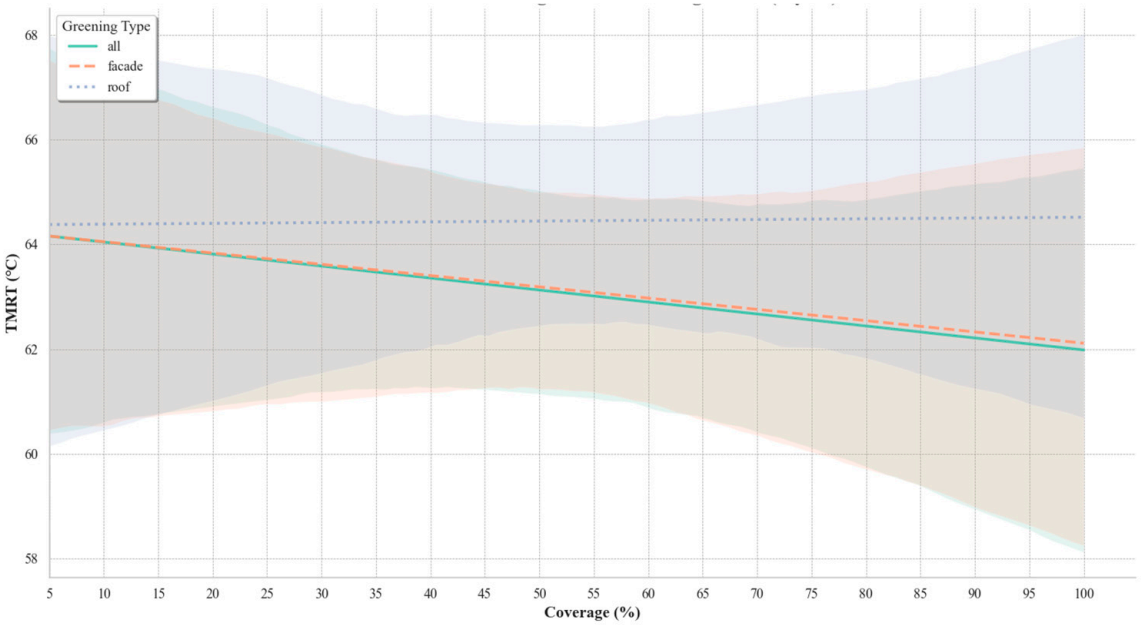

Figure 10. Mean radiation temperature levels with regression.

3.2.3. Physiological Equivalent Temperature

The effect of different green coverage and green types on PET in the community is shown in Figure 11. Compared with the mean radiation temperature and air temperature, PET, as an important indicator of comprehensive human thermal comfort, is not only affected by radiation and air temperature, but also integrates a variety of factors, such as wind speed and humidity, so its daily rule of change and greening regulation effect is more complex [51]. In general, the daily PET trends were similar to the mean radiant temperature. At low coverage (5–30%), the PET of all three types of greenery was close to 57.5 °C at midday, which corresponds to the "extreme heat stress" level, indicating that greenery has limited ability to ameliorate heat stress at low coverage. Of these, ALL types are only about 0.3 °C cooler than ROOF and FACADE, and greening is not sufficient to significantly mitigate extreme midday heat stress. In the morning and evening, PET remained at 42.2–45.6 °C, all in the "strong heat stress" category, with no significant differences between types. As the coverage increased to a medium level (35–70%), the PETs of the three greening types began to diverge. At midday, PET for ALL types decreased to about 54.5 °C, corresponding to a decrease from "extreme heat stress" to the "strong heat stress" boundary, which is about 1.2 °C and 0.7 °C lower than ROOF and FACADE, respectively, suggesting a greater potential for full-scale greening in mitigating This suggests that total greening has a greater potential for mitigating extreme heat stress at midday. The FACADE type is second to ALL but superior to ROOF in terms of cooling effect due to reduced wall radiation. The cooling advantage of the ALL type was further extended when entering high coverage (75–100%). At 100% coverage, the midday PET dropped to about 52.3 °C, which was close to the lower limit of "strong heat stress", while the PET of ROOF and FACADE were 53.2 °C and 54.3 °C, respectively, which were still at the upper limit of "strong heat stress". This suggests that comprehensive greening, through synergistic effects (e.g., shading and evapotranspiration effects), can significantly improve the thermal environment under high-coverage conditions, especially during the midday hours when the mitigation of heat stress is most effective.

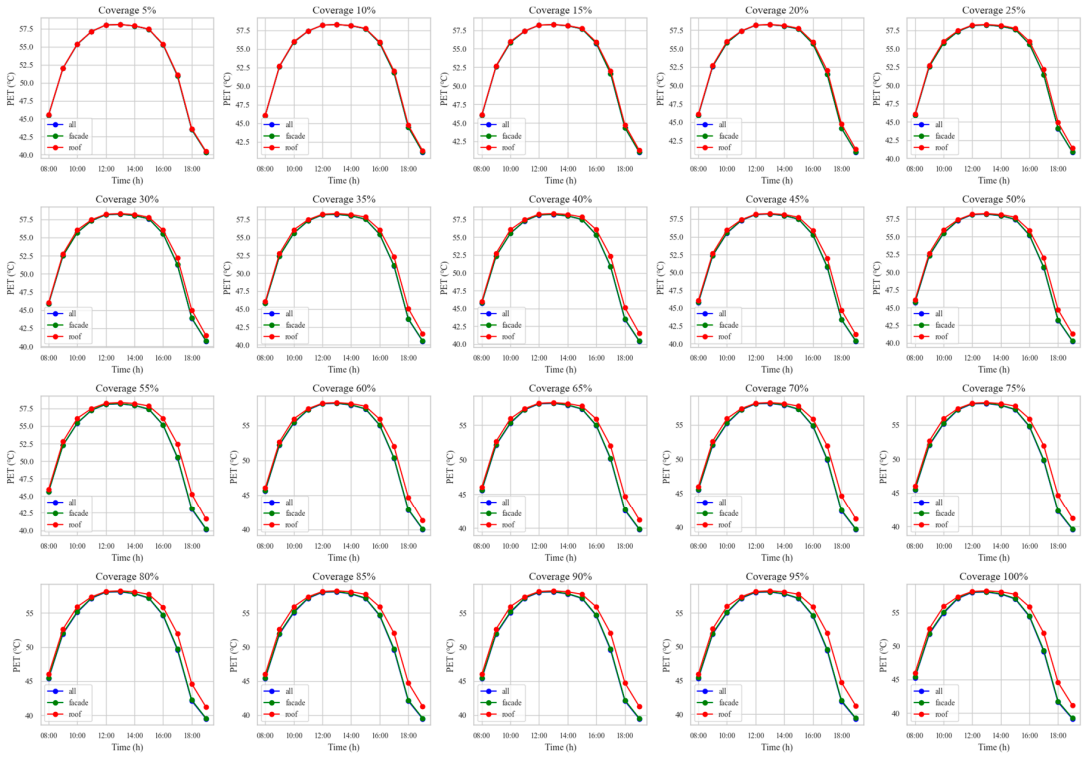

Figure 11. Effects of greening forms on the physiological equivalent temperature of communities with different percentages of coverage.

The time-by-time variability analysis of physiological equivalent temperature is shown in Figure 12. Significant differences ($p < 0.05$) were found between all greening forms and green roof forms, and between all greening forms and green facade forms at all time points, indicating that all greening forms performed well in improving thermal comfort. The effect was most pronounced during the midday hours (12:00–15:00) when all green forms were more effective in reducing PET, with p-values typically below 0.01. However, comparisons between facades and roofs were not as pronounced, with p-values close to or higher than 0.05 at certain times of day, e.g., early morning (8:00) and late evening (17:00). This suggests that, while facades and roofs had a limited effect, the fully enclosed form provided the most significant improvement in PET, especially during high heat periods.

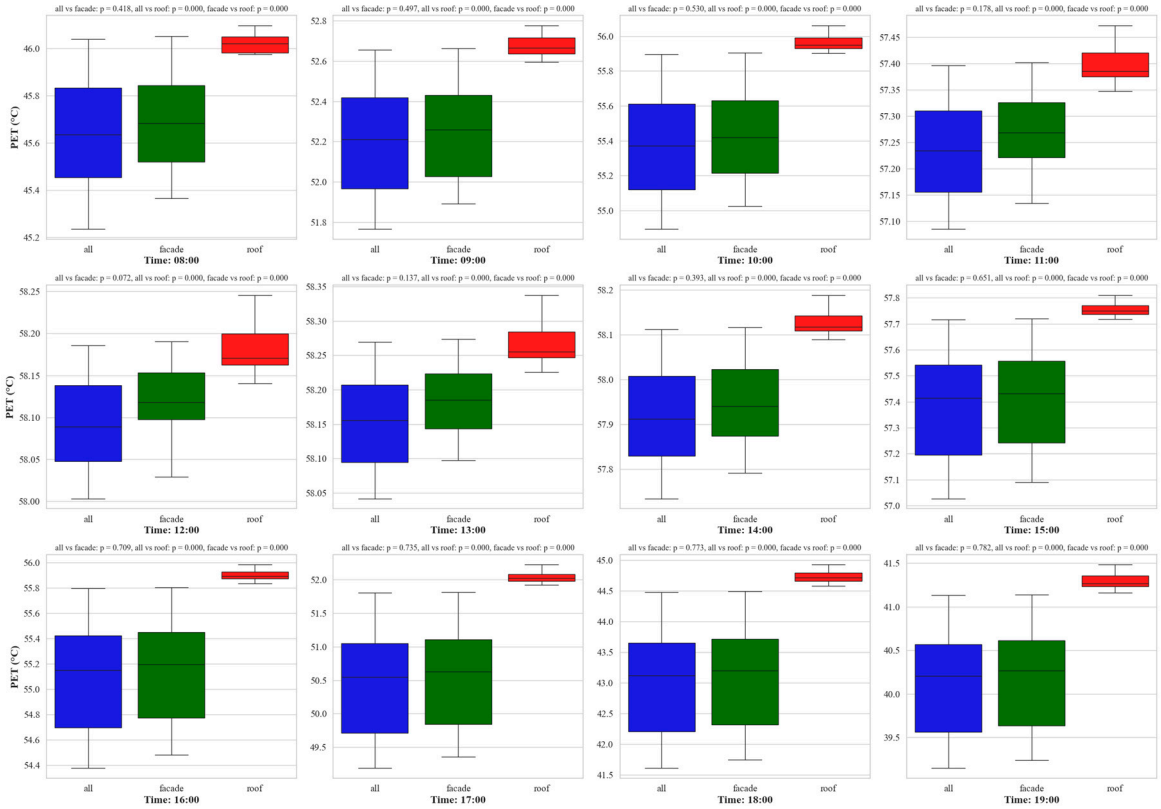

Figure 12. Variability analysis of physiological equivalent temperature in different greening types.

The overall regression relationship between coverage and PET is shown in Figure 13. ALL types have resulted in an average decrease in PET of about 2.5 °C, from 53.5 °C to 51.1 °C, over the course of the coverage from 5% to 100%. This performance shows that total greening can significantly mitigate heat stress at higher cover rates, especially when the cover rate exceeds 50%, and PET gradually moves from the "extreme heat stress" to the "strong heat stress" boundary. In contrast, the FACADE type was slightly less effective, with PET decreasing from 53.8 °C to 52.3 °C, an average decrease of about 1.5 °C. This suggests that vertical greening has a limited effect on PET by reducing wall heat radiation, especially at less than 50% coverage. This suggests that vertical greening has a limited effect on PET by reducing thermal radiation from the wall, especially at less than 50% coverage, and its cooling effect is similar to that of ROOF, which only slightly improves the "extreme heat stress" environment. ROOF type has the weakest cooling capacity, with the PET decreasing by only about 1.9 °C (from 54.1 °C to 53.1 °C) when going from 5% to 100% coverage, and the thermal stress level is always maintained at the boundary of "extreme thermal stress". In particular, it should be noted that when the coverage exceeded 75%, the PET of ALL type dropped to 51.0 °C, which was 0.4 °C above the lower limit of "strong heat stress", while the FACADE and ROOF were still higher than 52 °C. This suggests that

under high coverage, comprehensive greening can more effectively reduce PET to near the boundary of "strong heat stress" through the integrated regulation of thermal radiation and evapotranspiration cooling.

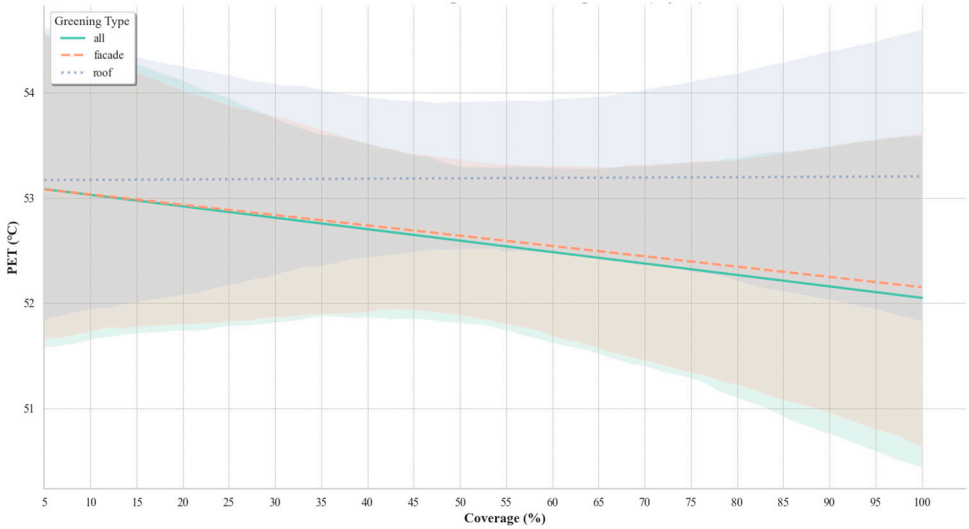

Figure 13. Physiological equivalent temperature levels with regression.

Green facades and green roofs have limited effectiveness in reducing temperatures, mainly due to limitations in their coverage and evapotranspiration. The green facade only covers the building wall, mainly reducing the absorption of heat radiation on the wall surface, but its scope of action affects the local space immediately adjacent to the wall to a greater extent, while the green roof mainly acts on the top of the building, improving the air temperature at the top by reducing the heat load on the roof, but its evapotranspiration is concentrated in the high altitude, and it is difficult to effectively infiltrate to the height of the pedestrians [52]. In addition, single green facade and green roof measures lack the synergy to regulate heat radiation from walls and roofs at the same time, making their overall cooling effect much less effective than ALL types [53]. The directionality of solar radiation further limits the performance of green walls, with differently oriented walls resulting in uneven shading due to different angles of radiation, and green roofs having a weak indirect effect on wall radiation [46]. Therefore, these two single greening measures have limited potential to improve the thermal environment of high-density communities, and perform less effectively than the synergistic cooling effect of comprehensive greening.

4. Discussion

4.1. Comparison with Other Studies

The results of this study highlight the significant cooling effect of all-around greening at different levels of cover, in line with the wider literature on green facades, and also extend existing knowledge by demonstrating the superior performance of all-around greening (ALL types) across a range of time periods and cover conditions.

Existing studies similarly emphasize the cooling potential of green facades. For example, experiments conducted in Mediterranean climates revealed that the temperatures behind green facades could be up to 7 °C cooler than those behind shade sails, with evapotranspirative cooling contributing significantly to gap cooling [21]. However, these studies primarily focused on localized wall and gap cooling effects rather than comprehensive community-scale impacts. Furthermore, research in composite climates, such as New Delhi [54], demonstrated temperature reductions of up to 8.1 °C on southwest-oriented facades during peak afternoon hours, yet these benefits were accompanied by increased relative humidity, potentially impacting thermal comfort—an effect less pronounced in the

current study's findings due to the broader scope of coverage and integration of horizontal and vertical greening.

Another noteworthy comparison is the effect of building materials on the cooling performance of building-attached greening. The modular double-glazed green facade reduced indoor temperatures by up to 4.9 °C [20]. While these systems optimize building-specific cooling through innovative integration, their impacts are inherently localized. Instead, the community-scale focus of this study emphasizes the broader applicability of green infrastructure to urban heat mitigation.

Collectively, these findings highlight the diverse mechanisms—evapotranspiration, shading, and heat load reduction—through which green facades and greening strategies influence thermal performance. While facade-specific studies provide critical insights into building-scale cooling, the current study offers valuable evidence for the scalability and enhanced effectiveness of comprehensive greening systems, particularly under high-coverage conditions. This suggests that a holistic approach, combining vertical and horizontal greening, can achieve superior thermal regulation, making it a more effective strategy for urban climate adaptation.

4.2. Planning Understanding and Recommendations

First, comprehensive greening (ALL type) should be the priority option for greening design in urban villages. Total greening minimizes direct heating of buildings by solar radiation through double coverage of roofs and walls while enhancing the ability of evapotranspiration to regulate local microclimates. Under high coverage conditions ($\geq$75%), comprehensive greening can significantly reduce the PET at a pedestrian height of 1.5 m, which, to a certain extent, can alleviate the "extreme heat stress" caused by high temperatures in summer and provide a more comfortable thermal environment for residents. Therefore, it is recommended to promote the integrated model of "rooftop greening + vertical greening" in the transformation of urban villages to optimize its effect on thermal comfort.

Second, vertical greening (FACADE type) is more maneuverable in the small space of urban villages and should be an important complementary measure. Since roofs in urban villages are often used for living and economic purposes (e.g., drying, storage), there may be some limitations in implementing roof greening, whereas vertical greening does not take up additional space and can be realized by simply attaching to the wall. Vertical greening can significantly reduce thermal radiation from walls, especially in communities with a high density of high-rise buildings, and by optimizing orientation and greening layout, it can effectively mitigate the negative impact of wall surfaces on the surrounding thermal environment.

In addition, green roofs (ROOF types) remain relevant as a complementary measure. Although its direct improvement of the thermal environment at pedestrian heights is limited, green roofs can indirectly reduce the energy consumption of indoor air conditioning by reducing the internal heat load of the building, easing the pressure on energy consumption in the community as a whole. At the same time, green roofs can also be used as part of stormwater management to reduce the pressure on the drainage system within the community by increasing vegetation cover and improving the retention and infiltration capacity of stormwater.

4.3. Limitations

Although this study explored the effect of greening on the thermal environment at 1.5 m pedestrian height in urban villages in Guangzhou City from the perspectives of different coverage and greening types (ALL, FACADE, and ROOF), there are still some limitations. First, the study is based on simulation results. While the model incorporates key factors such as radiation, evapotranspiration, and heat transfer, the actual cooling effects in complex urban village environments may deviate due to uncontrollable factors such as microclimatic conditions, building material properties, and wind environments. Second, the

study assumed an idealized uniform distribution of green coverage. However, in practice, greenery distribution is often uneven due to the complex spatial layout of urban villages, which may lead to spatial variations in cooling effects not fully captured in the simulations. Moreover, challenges such as economic feasibility, structural limitations, and the need for maintenance significantly impact the practical implementation of green infrastructure in high-density urban villages. These factors can hinder large-scale adoption and limit the effectiveness of greening interventions. In addition, the study did not consider seasonal variations in vegetation, which significantly influence urban microclimates. Finally, the field measurements were conducted in a typical high-density urban village in Guangzhou, which may increase the uncertainty of applying the study results to other urban villages with different densities and layouts. Future studies should be extended to more diverse urban villages and incorporate real-world field data to validate and optimize the model. In summary, future research should explore spatial optimization strategies, the long-term dynamics of greening, and comprehensive assessments of microclimate improvements to enhance the practical applications of greening strategies.

5. Conclusions

This study investigated the synergistic cooling effect of roof greening and façade/vertical greening in urban villages, a subtropical high-density community in Guangzhou City. The study is based on a simulated dataset and provides scientific evidence for the thermal benefits of integrated greening strategies under different green cover conditions. An in-depth analysis of the green coverage thresholds required to achieve significant urban cooling and enhanced thermal comfort, as well as the impact of different greening forms on the thermal environment at pedestrian heights, is provided by the validated ENVI-met model. In particular, we explore the advantages of total greening (combined roof and wall greening) over single facade greening or roof greening, as well as the differences in the cooling effects of the three types of greening at different coverage rates.

The results of this study show that in order to significantly improve thermal comfort at a pedestrian height of 1.5 m in a high-density environment of urban villages in Guangzhou City, green coverage of more than 50% is required, and full greening (ALL types) can reduce the PET by about 2 °C during the midday hours, and at the same time reduce the heat stress level by one level (from “extreme heat stress” to “strong heat stress”). Vertical greening (FACADE type) is more significant in regulating the thermal environment of the community, especially under high coverage conditions, and its effect is close to that of full-scale greening, while green roofs (ROOF type) are relatively weak in cooling capacity. In addition, this study found that comprehensive greening significantly increased the cooling potential at more than 75% coverage, while a single form of greening provided more limited improvement in thermal comfort at less than 50% coverage.

This study further shows that while green coverage is an important factor in improving the thermal environment, the choice of green form and spatial configuration is equally critical. Total greening is the best strategy for greening design in high-density urban villages because it can significantly amplify the thermal benefits through the synergistic effect on walls and roofs. However, in actual planning, it is not practical to rely on a single comprehensive greening strategy due to the limited space and dense buildings in urban villages. Therefore, it is recommended that greening types be flexibly arranged in combination with vertical greening and rooftop greening features to maximize their thermal environment improvement potential. In addition, other strategies, such as climate-sensitive building design, optimizing community ventilation, and incorporating ground-level greening, should be innovatively integrated into the planning and design of urban villages, especially in subtropical climatic zones, in order to comprehensively reduce the heat load of high-density urban communities and to enhance the living comfort and sustainable development of residents.

Author Contributions: Conceptualization, C.L.; Methodology, C.L.; Software, C.L.; Validation, C.L.; Formal analysis, C.L.; Investigation, C.L.; Resources, S.Z.; Data curation, S.Z.; Writing—original draft, C.L.; Writing—review & editing, S.Z.; Visualization, S.Z.; Supervision, S.Z.; Project administration, S.Z.; Funding acquisition, S.Z. All authors have read and agreed to the published version of the manuscript.

Funding: This research was funded by the "Guangzhou Philosophy and Social Science Development 14th Five-Year Plan Project" (grant number 2022GZYB67) and the Guangdong Science and Technology Department "Guangzhou Academy of Fine Arts—Art and Science Support Platform".

Data Availability Statement: The data presented in this study are available on request from the corresponding author.

Conflicts of Interest: The authors declare no conflict of interest.

References

1. Li, Y.H.; Jia, L.R.; Wu, W.H.; Yan, J.Y.; Liu, Y.S. Urbanization for rural sustainability—Rethinking China's urbanization strategy. *J. Clean. Prod.* **2018**, *178*, 580–586. [CrossRef]
2. Guo, J.; Xia, D.; Zhang, L.; Zou, Y.; Guo, G.; Chen, Z.; Xie, W. Assessing the winter indoor environment with different comfort metrics in self-built houses of hot-humid areas: Does undercooling matter for the elderly? *Build. Environ.* **2024**, *263*, 111871. [CrossRef]
3. Zhang, L.Z.; Ye, Y.M.; Wang, J.J. Influential Factors and Geographical Differences in the Redevelopment Willingness of Urban Villagers: A Case Study of Guangzhou, China. *Land* **2022**, *11*, 233. [CrossRef]
4. Yang, J.; Zhao, Y.; Zou, Y.; Xia, D.; Lou, S.; Guo, T.; Zhong, Z. Improving the Thermal Comfort of an Open Space via Landscape Design: A Case Study in Hot and Humid Areas. *Atmosphere* **2022**, *13*, 1604. [CrossRef]
5. Guo, T.; Lin, Z.; Zhao, Y.; Fang, Z.; Fan, Y.; Zhang, X.; Yang, J.; Li, Y. Investigation and optimization of outdoor thermal comfort in elementary school campuses: Example from a humid-hot area in China. *Build. Environ.* **2024**, *248*, 111055. [CrossRef]
6. Ciacci, C.; Banti, N.; Di Naso, V.; Montechiaro, R.; Bazzocchi, F. Experimentation of Mitigation Strategies to Contrast the Urban Heat Island Effect: A Case Study of an Industrial District in Italy to Implement Environmental Codes. *Atmosphere* **2022**, *13*, 1808. [CrossRef]
7. Ribeiro, F.P.; Oladimeji, O.; de Mendonça, M.B.; Boer, D.; Maqbool, R.; Haddad, A.N.; Najjar, M.K. BIM-based parametric energy analysis of green building components for the roofs and facades. *Next Sustain.* **2025**, *5*, 100078. [CrossRef]
8. Bakhshoodeh, R.; Ocampo, C.; Oldham, C. Impact of ambient air temperature, orientation, and plant status on the thermal performance of green façades. *Energy Build.* **2023**, *296*, 113389. [CrossRef]
9. Bochenek, A.D.; Klemm, K. The Impact of Passive Green Technologies on the Microclimate of Historic Urban Structures: The Case Study of Lodz. *Atmosphere* **2020**, *11*, 974. [CrossRef]
10. Zhao, Y.; Yang, J.; Fang, Z.; Zhang, X.; Guo, T.; Li, Y. Passive design strategies to improve student thermal comfort: A field study in semi-outdoor spaces of academic buildings in hot-humid areas. *Urban Clim.* **2024**, *53*, 101807. [CrossRef]
11. Alexandri, E.; Jones, P. Temperature decreases in an urban canyon due to green walls and green roofs in diverse climates. *Build. Environ.* **2008**, *43*, 480–493. [CrossRef]
12. Wong, N.H.; Tan, A.Y.K.; Tan, P.Y.; Wong, N.C. Energy simulation of vertical greenery systems. *Energy Build.* **2009**, *41*, 1401–1408. [CrossRef]
13. de Jesus, M.P.; Lourenço, J.M.; Arce, R.M.; Macias, M. Green façades and in situ measurements of outdoor building thermal behaviour. *Build. Environ.* **2017**, *119*, 11–19. [CrossRef]
14. Morakinyo, T.E.; Lai, A.; Lau, K.K.-L.; Ng, E. Thermal benefits of vertical greening in a high-density city: Case study of Hong Kong. *Urban For. Urban Green.* **2019**, *37*, 42–55. [CrossRef]
15. Tan, C.L.; Wong, N.H.; Jusuf, S.K. Effects of vertical greenery on mean radiant temperature in the tropical urban environment. *Landsc. Urban Plan.* **2014**, *127*, 52–64. [CrossRef]
16. Onishi, A.; Cao, X.; Ito, T.; Shi, F.; Imura, H. Evaluating the potential for urban heat-island mitigation by greening parking lots. *Urban For. Urban Green.* **2010**, *9*, 323–332. [CrossRef]
17. Liang, H.H.; Huang, K.T. Study on rooftop outdoor thermal environment and slab insulation performance of grass planted roof. *Int. J. Phys.* **2011**, *6*, 65–73.
18. Scherba, A.; Sailor, D.J.; Rosenstiel, T.N.; Wamser, C.C. Modeling impacts of roof reflectivity, integrated photovoltaic panels and green roof systems on sensible heat flux into the urban environment. *Build. Environ.* **2011**, *46*, 2542–2551. [CrossRef]
19. Qahtan, A.M. Thermal conditions in workspace centre and adjacent to inclined glazed façade of a green-certified office building in the tropics. *Case Stud. Therm. Eng.* **2024**, *53*, 103798. [CrossRef]
20. Bao, S.; Zou, S.; Li, B.; Chen, Q.; Zhao, M. Experiments on the cooling effect of modular vertical greening on double-glazed façade in summer. *Build. Environ.* **2022**, *226*, 109771. [CrossRef]
21. Bakhshoodeh, R.; Ocampo, C.; Oldham, C. Exploring the evapotranspirative cooling effect of a green façade. *Sustain. Cities Soc.* **2022**, *81*, 103822. [CrossRef]

22. Pan, W.; Du, J. Towards sustainable urban transition: A critical review of strategies and policies of urban village renewal in Shenzhen, China. *Land Use Policy* **2021**, *111*, 105744. [CrossRef]
23. Gong, Y.; Li, B.; Tong, D.; Que, J.; Peng, H. Planner-led collaborative governance and the urban form of urban villages in redevelopment: The case of Yangji Village in Guangzhou, China. *Cities* **2023**, *142*, 104521. [CrossRef]
24. Yang, J.; Zhao, Y.; Wan, Z.F. The impact of tree species and planting location on outdoor thermal comfort of a semi-outdoor space. *Int. J. Biometeorol. J. Int. Soc. Biometeorol.* **2023**, *67*, 1689–1701. [CrossRef] [PubMed]
25. Zhang, Y.; Zheng, Z.; Zhang, S.; Fang, Z.; Lin, Z. Exploring Thermal Comfort and Pleasure in Outdoor Shaded Spaces: Inspiration for Improving Thermal Index Models. *Build. Environ.* **2024**, *265*, 111933. [CrossRef]
26. Fang, Z.; Zhang, F.; Guo, Z.; Zheng, Z.; Feng, X. Investigation into the outdoor thermal comfort on different urban underlying surfaces. *Urban Clim.* **2024**, *55*, 101911. [CrossRef]
27. Zhang, S.; Zhang, X.; Niu, D.; Fang, Z.; Chang, H.; Lin, Z. Physiological equivalent temperature-based and universal thermal climate index-based adaptive-rational outdoor thermal comfort models. *Build. Environ.* **2023**, *228*, 109900. [CrossRef]
28. Tang, T.; Zhou, X.; Zhang, Y.; Feng, X.; Liu, W.; Fang, Z.; Zheng, Z. Investigation into the thermal comfort and physiological adaptability of outdoor physical training in college students. *Sci. Total Environ.* **2022**, *839*, 155979. [CrossRef] [PubMed]
29. Fang, Z.; Feng, X.; Xu, X.; Zhou, X.; Lin, Z.; Ji, Y. Investigation into outdoor thermal comfort conditions by different seasonal field surveys in China, Guangzhou. *Int. J. Biometeorol.* **2019**, *63*, 1357–1368. [CrossRef]
30. Yang, J.Y.; Hu, X.Y.; Feng, H.Y.; Marvin, S. Verifying an ENVI-met simulation of the thermal environment of Yanzhong Square Park in Shanghai. *Urban For. Urban Green.* **2021**, *66*, 127384. [CrossRef]
31. Liu, Z.X.; Cheng, K.Y.; Sinsel, T.; Simon, H.; Jim, C.Y.; Morakinyo, T.E.; He, Y.Y.; Yin, S.; Ouyang, W.L.; Shi, Y.; et al. Modeling microclimatic effects of trees and green roofs/façades in ENVI-met: Sensitivity tests and proposed model library. *Build. Environ.* **2023**, *244*, 110759. [CrossRef]
32. Liu, Z.X.; Cheng, W.W.; Jim, C.Y.; Morakinyo, T.E.; Shi, Y.; Ng, E. Heat mitigation benefits of urban green and blue infrastructures: A systematic review of modeling techniques, validation and scenario simulation in ENVI-met V4. *Build. Environ.* **2021**, *200*, 107939. [CrossRef]
33. Tsoka, S.; Tsikaloudaki, A.; Theodosiou, T. Analyzing the ENVI-met microclimate model's performance and assessing cool materials and urban vegetation applications-A review. *Sustain. Cities Soc.* **2018**, *43*, 55–76. [CrossRef]
34. Middel, A.; Häb, K.; Brazel, A.J.; Martin, C.A.; Guhathakurta, S. Impact of urban form and design on mid-afternoon microclimate in Phoenix Local Climate Zones. *Landsc. Urban Plan.* **2014**, *122*, 16–28. [CrossRef]
35. Lee, H.; Mayer, H.; Chen, L. Contribution of trees and grasslands to the mitigation of human heat stress in a residential district of Freiburg, Southwest Germany. *Landsc. Urban Plan.* **2016**, *148*, 37–50. [CrossRef]
36. Liu, Z.X.; Zheng, S.L.; Zhao, L.H. Evaluation of the ENVI-Met Vegetation Model of Four Common Tree Species in a Subtropical Hot-Humid Area. *Atmosphere* **2018**, *9*, 198. [CrossRef]
37. Lin, C.; Wu, Z.T.; Li, H.; Huang, J.; Huang, Q.L. Comprehensive analysis on the thermal comfort of various greening forms: A study in hot-humid areas. *Environ. Res. Commun.* **2024**, *6*, 025010. [CrossRef]
38. Guo, T.Y.; Zhao, Y.; Yang, J.H.; Zhong, Z.N.; Ji, K.F.; Zhong, Z.Y.; Luo, X.Y. Effects of Tree Arrangement and Leaf Area Index on the Thermal Comfort of Outdoor Children's Activity Space in Hot-Humid Areas. *Buildings* **2023**, *13*, 214. [CrossRef]
39. China Statistics Press. *China Statistical Yearbook*; China Statistics Press: Beijing, China, 2023.
40. Wen-Cui, Q.; Dan, H.U.; Yuan-Zheng, L.I.; Zhen, G. Numerical simulation of microclimate in Beijing typical residential area based on ENVI-met model. *J. Meteorol. Environ.* **2015**, *31*, 56–62.
41. Elnabawi, M.H.; Hamza, N.; Dudek, S. Use and Evaluation of the Envi-Met Model for Two Different Urban Forms in Cairo, Egypt: Measurements and Model Simulations. In Proceedings of the 13th Conference of International Building Performance Simulation Association, Chambéry, France, 26–28 August 2013.
42. Liu, Z.; Zheng, S.; Fang, X.; Lu, X.; Zhao, L. Simulating validation of ENVI-met vegetation model to Ficus microcarpa in hot-humid region of subtropical zone. *Beijing Linye Daxue Xuebao/J. Beijing For. Univ.* **2018**, *40*, 1–12.
43. Yingxue, C.; Beibei, G.; Xuemin, W.K. Assessment of urban blue-green space cooling effect linking maximum and accumulative perspectives in the Yangtze River Delta, China. *Environ. Sci. Pollut. Res.* **2023**, *30*, 121834–121850.
44. Hendarti, R. The Influence of the Evapotranspiration Process of Green Roof Tops on PV Modules in the Tropics. Ph.D. Thesis, National University of Singapore, Singapore, 22 August 2013.
45. Amjad, K. Construction and design requirements of green buildings' roofs in Saudi Arabia depending on thermal conductivity principle. *Constr. Build. Mater.* **2018**, *186*, 1119–1131.
46. Blanco, I.; Convertino, F.; Schettini, E.; Vox, G. Energy analysis of a green facade in summer: An experimental test in Mediterranean climate conditions. *Energy Build.* **2021**, *245*, 111076. [CrossRef]
47. Perez, G.; Coma, J.; Chafer, M.; Cabeza, L.F. Seasonal influence of leaf area index (LAI) on the energy performance of a green facade. *Build. Environ.* **2022**, *207*, 108497. [CrossRef]
48. Peng, L.; Jim, C. Green-Roof Effects on Neighborhood Microclimate and Human Thermal Sensation. *Energies* **2013**, *6*, 598–618. [CrossRef]
49. Schindler, B.Y.; Blaustein, L.; Vasl, A.; Kadas, G.J.; Seifan, M. Cooling effect of Sedum sediforme and annual plants on green roofs in a Mediterranean climate. *Urban For. Urban Green.* **2019**, *38*, 392–396. [CrossRef]

50. Malys, L.; Musy, M.; Inard, C. Direct and Indirect Impacts of Vegetation on Building Comfort: A Comparative Study of Lawns, Green Walls and Green Roofs. *Energies* **2017**, *9*, 32. [CrossRef]
51. Ren, Z.B.; Fu, Y.; Dong, Y.L.; Zhang, P.; He, X.Y. Rapid urbanization and climate change significantly contribute to worsening urban human thermal comfort: A national 183-city, 26-year study in China. *Urban Clim.* **2022**, *43*, 101154. [CrossRef]
52. Guo, X.; Chen, X.; Yu, Y.; Wei, S.; Chen, W. A simplified modeling method for studying the thermal performance of buildings with vertical greening systems. *J. Clean. Prod.* **2024**, *467*, 142940. [CrossRef]
53. Raji, B.; Tenpierik, M.J.; Andy, V.D.D. The impact of greening systems on building energy performance: A literature review. *Renew. Sustain. Energy Rev.* **2015**, *45*, 610–623. [CrossRef]
54. Nagdeve, S.S.; Manchanda, S.; Dewan, A. Thermal performance of indirect green façade in composite climate of India. *Build. Environ.* **2023**, *230*, 109998. [CrossRef]